

Nanoscale Fe-based Catalysts from Laser Pyrolysis

P. C. Eklund, Xiang-Xin Bi, and F. J. Derbyshire
Center for Applied Energy Research
University of Kentucky
Lexington, KY 40511-8433

Keywords: Ultrafine particle, catalyst, coal liquefaction, laser pyrolysis

Introduction

Iron-based catalysts have been extensively investigated for their catalytic behavior in direct coal liquefaction^[1]. Although they are generally less active than other catalysts containing transition metals such as molybdenum, vanadium, etc, they are favored for economical reasons. The catalytic activity of these iron-based catalysts depends mainly on their chemical composition and effective contact area with the coal-solvent slurry. The contact area relates closely to the particle diameter, surface morphology, and particle agglomeration. Research to produce nanoscale (~10 nm dia.) ultrafine particle (UFP) catalysts with *controllable* chemical composition and particle size is of fundamental importance to study the effect of these factors on the catalytic activity.

In this paper, we report the results of a study to synthesize and characterize nanoscale (5-20nm) UFP Fe-based catalysts for direct coal liquefaction. The UFPs were produced by the laser-driven gas phase reaction of $\text{Fe}(\text{CO})_5$ with C_2H_4 . By adjusting the reaction conditions we have found it possible to produce reasonably pure phase (~95%) batches of $\alpha\text{-Fe}$, Fe_3C and Fe_7C_3 particles with a size distribution of ~2-4 nm. Typical production rates are ~1 g/hr. By adding H_2S to the reactant gas stream we have succeeded recently in producing UFP pyrrhotite (Fe_{1-x}S). Results from our studies to determine the catalytic benefit of UFP Fe-carbide catalysts in coal liquefaction have produced some promising results^[2]. These experiments were carried out in a microautoclave with dimethyl disulfide (DMDS) added to improve conversion to iron sulfide. Our studies have shown that, under liquefaction conditions, the UFP Fe-carbide catalysts are transformed into pyrrhotite. This transformation complicates the identification of the active catalyst phase and, of course, raises questions about the activity and the role of the carbides in the conversion of coal into liquids and gases. Our recent success in synthesizing UFP pyrrhotite should allow us to study these questions, as well as evaluate the activity of UFP Fe_{1-x}S .

We have characterized the physical properties of our UFP catalysts by X-ray diffraction (XRD), optical spectroscopy (reflectivity and Raman scattering),

transmission and scanning electron microscopy (TEM and SEM) and ^{57}Fe Mossbauer spectroscopy.

The CO_2 laser pyrolysis technique, invented by Haggerty et al.^[3], has been established as a useful technique for the synthesis of ultrafine particles (UFP) in the size range 5 - 30 nm. In the past, a variety of UFPs have been produced using this technique; they include $\{\text{Si}, \text{SiC}, \text{Si}_3\text{N}_4\}$ ^[3], $\{\text{ZrB}_2, \text{TiO}_2\}$ ^[4], Fe_3C ^[5], $\{\text{WC}, \text{MoS}_2\}$ ^[6]. These UFPs (e.g., SiC and Si_3N_4) have been found to be free from contamination and exhibit a narrow particle size distribution^[3]. The synthesis of UFP Fe_3C using laser pyrolysis was first explored by Fiato et al. at Exxon^[5]. They proposed a basic chemical reaction involving the thermal decomposition of $\text{Fe}(\text{CO})_5$ and subsequent reaction with C_2H_4 at high temperature sustained by CO_2 laser illumination which couples strongly to the vibrational bands of C_2H_4 . They found that UFP Fe_3C forms as a product of this process. Fiato et al.^[5] demonstrated that the particle composition, i. e., carbon to iron ratio, could be controlled by varying the preparation conditions. Prior to our work, no studies have been reported which correlate the reaction parameters with particle size, chemical composition or crystalline phase. Furthermore, the Exxon group did not report the formation of Fe_7C_3 , which exhibits a hexagonal structure^[12].

Experiment

Our laser pyrolysis system^[3-5, 7, 8] is shown schematically in Fig. 1. The reactant gases flow vertically out of a stainless steel tube with a nozzle of area A. Studies of the effect of A on particle production have been carried out over the range $A \sim 2 - 5 \text{ mm}^2$. The pyrolysis reaction zone is formed at the intersection of the horizontal infrared beam from a continuous (CW) CO_2 laser, tuned at the P20 line, and the vertical flow of reactant gases from the nozzle. The reactant gases and associated particle growth are confined within the reaction zone by a coaxial flow of Ar gas which passed through a larger tube concentric with the much smaller reactant gas tube (Fig. 1). Argon gas is also introduced into the entrance and exit windows in such a way as to continually sweep any stray particles off the NaCl windows (Fig. 1). Mass flow controllers are used to establish steady gas flows of Ar, and to regulate the flow of C_2H_4 (2-30 sccm) and H_2S (2-20 sccm). The total pressure in the cell was controlled by a needle valve located between a rotary vacuum pump and the stainless steel reaction chamber (6-way cross). Particles are collected downstream in a Pyrex trap indicated in Fig. 1. Since the $\alpha\text{-Fe}$, Fe_3C and Fe_7C_3 particles are ferromagnetic, we have employed a magnetic field to trap the particles using a stack of permanent magnets placed beneath the trap (Fig. 1).

The pyrrhotite Fe_{1-x}S UFPs were synthesized by adding H_2S to the C_2H_4

and $\text{Fe}(\text{CO})_5$ reactant gas stream, at a flow rate of 7 sccm. The other reaction parameters are set at the values which would otherwise produce α -Fe particles (Table 1). These sulfide particles are non-magnetic and are not attracted to the magnets beneath the collection trap (Fig. 1). As a result, the particles tend to drift toward the far end of the trap and clog the 0.2μ pore size membrane filter, which complicates the steady state production of these particles. Other means of trapping pyrrhotite particles are being investigated to solve this problem. It is interesting to speculate that the non-magnetic properties of pyrrhotite UFPs may lead to much less particle agglomeration compared to ferromagnetic carbide UFPs, and thus better dispersion in the coal slurry.

To handle most of our Fe-based UFPs in air, we have found it necessary to passivate the surface in situ in the collection trap. The passivation is carried out by flowing 4-10% O_2 -in- He_2 for several hours.

Results and Discussion

Shown in Fig. 2 are the XRD results for UFP α -Fe, Fe_3C and Fe_7C_3 using the reaction parameter values given in Table 1. In this figure, the dots represent experimental data and the lines are calculated using a sum of Lorentzian functions whose peak positions and relative strengths are obtained from published powder diffraction data^[9]. The same width parameter is used for all diffraction lines, and an exponential function is introduced to simulate the background. The Debye-Scherrer equation has been used to convert the X-ray line width into an average particle diameter. We find that these X-ray derived values for the particle diameter are in good agreement with Transmission Electron Microscopy (TEM) results, indicating that the UFPs are, for the most part, single crystal particles. The calculated diffraction pattern is seen to agree reasonably well with the data^[9], leading to our identification of the three phases as α -Fe, Fe_3C and Fe_7C_3 . The signature of Fe_3O_4 in the XRD data of α -Fe is believed to stem from the O_2 passivation.

We have found that higher chamber pressures (> 300 torr) and higher reactant gas flow rates (> 30 sccm) favor the formation of high carbon content crystalline phases such as Fe_7C_3 . On the other hand, lower chamber pressures and reactant gas flow rates favor the formation of α -Fe. A detailed study of the correlation between reaction parameter values and the associated solid UFP phases produced will appear elsewhere^[8]. Presented in Fig. 3a and 3b are, respectively, the XRD results for several batches of Fe_3C and Fe_7C_3 particles produced with different average particle sizes. The particle size indicated in the figure was estimated using the Debye-Scherrer equation^[13] and the data near $2\theta \sim 58^\circ$.

In Fig. 4, we show ^{57}Fe Mossbauer spectra collected at 12K for both Fe_3C and Fe_7C_3 . The solid line in Fig. 4 represents the calculated Mossbauer spectrum by fitting the data in the usual way. The results from the fit to room temperature data including internal magnetic field, isomer shift and quadruple splitting parameters are listed in Table 2. The parameter values for the Fe_3C particles at room temperature^[8] are compared with the results of Le Caer et al.^[11], and are found to be in good agreement. To our knowledge, Mossbauer results for Fe_7C_3 have not been reported. We find in this study that a model with four inequivalent magnetic sites is necessary to fit the data. Fe_7C_3 has three chemically inequivalent sites^[10]. Further Mossbauer and neutron scattering studies are underway to determine the magnetic structure of Fe_7C_3 UFPs.

Shown in Fig. 5 by the dotted lines are XRD data for iron sulfide (pyrrhotite) UFPs. For comparison, the solid lines in the figure represent the XRD data of Fe_7C_3 particles after reaction in our microautoclave with dimethyl disulfide(DMDS) at 375 °C. The vertical lines represent the standard powder diffraction intensities for pyrrhotite. As can be seen in the figure, the Fe-sulfide UFPs exhibit a diffraction pattern quite similar to pyrrhotite. However, on the basis of the XRD data, it is not possible to rule out that there may be significant incorporation of carbon into the UFP pyrrhotite lattice. Mossbauer studies are currently underway to address this point. One can also conclude from the XRD data in the figure that liquefaction conditions (and the presence of DMDS) rapidly converts UFP Fe-carbide into UFP pyrrhotite with slightly smaller particle size (and possibly with significant carbon content).

New results from coal liquefaction studies using nanoscale Fe-based catalysts, including UFP-pyrrhotite, will also be presented.

Acknowledgement

We thank Bhaswati Ganguly, Dr. Frank E. Huggins and Dr. Gerald P. Huffman for the Mossbauer studies. This work is supported by DOE Advanced Concepts, DE-AC22-91PC91040.

References

1. Derbyshire, Frank J., *Catalysis in Coal Liquefaction: New Direction for Research*(1988) IEA Coal Research, p. 2
2. Hager, Bi, Derbyshire, Eklund, Stencil, "Ultrafine Iron Carbide as Liquefaction Catalyst Precursor", ACS Preprints- Division of Fuel Chemistry, 36(4) 1900-8(1991)
3. J. S. Haggerty, *Sinterable Powders from Laser-Driven Reactions*, in *Laser-induced Chemical Processes*, J.I. Steinfeld, Editor. 1981, Plenum Press: New York.
4. G. W. Rice, and R. L. Woodin, J. Am. Ceram. Soc., 1988. 71 : p. C181.
5. R. A. Fiato, G. W. Rice, S. Miseo, and S. L. Soled, United States Patent, 1987. **4,637,753**.
6. R. A. Fiato, G. W. Rice, and S. L. Soled, U. S. Patents, 1988. **4659681, 4668647**.
7. G. W. Rice, and et al., United States Patent, 1987. **4,659,681**.
8. G. W. Rice, and R. L. Woodin. *Applications of Lasers to Industrial*. in *SPIE*. 1984.
9. Powder Diffraction File of the Joint Committee on Powder Diffraction Standard(International Center for Diffraction Data, Swarthmore, PA, 1991).
10. Xiang-Xin Bi, P. C. Eklund, et al., in preparation.
11. R. L. Cohen, *Applications of Mossbauer Spectroscopy*. ed. R.L. Cohen, 1980, New York: Academic Press.
12. H. L. Yakel, International Metals Reviews, 1985. **30**: p. 17.
13. B. D. Cullity, *Elements of X-Ray Diffraction*. 1967, Addison-Wesley Publishing Company, Inc.

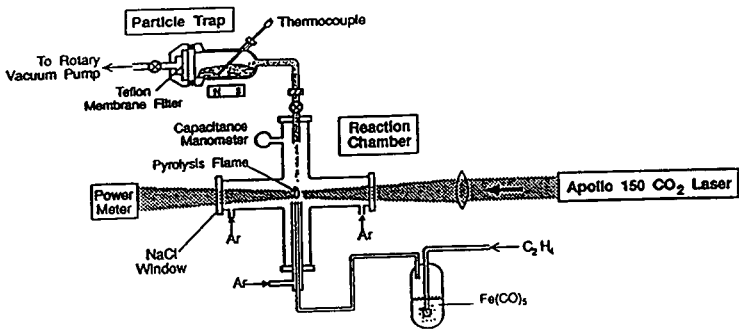
Table 1 Typical laser pyrolysis reaction parameters.

	α -Fe	Fe ₃ C	Fe ₇ C ₃
Laser Intensity(W)	30	50	54
Beam Width(mm)	1	1	0.2
Nozzle Diameter(mm)	1.7	0.8	0.8
Chamber Pressure(Torr)	100	300	500
C ₂ H ₄ Flow Rate(sccm)	9	9	25

Table 2 Room-temperature ⁵⁷Fe Mossbauer parameters including hyperfine magnetic splitting(H₀), isomer shift(I. S.) and quadropole splitting(Q. S.) for UFP Fe₃C and Fe₇C₃.

	H ₀ (KG)	I. S. (mm/s)	Q. S. (mm/s)
Fe ₇ C ₃ *	228	0.32	-0.17
	210	0.23	0.03
	185	0.20	-0.04
Fe ₃ C*	163	0.21	0.07
	210	0.19	0.02
Fe ₃ C ⁽¹¹⁾	198	0.19	0.01
	208	0.18	0.02
	206	0.18	0.02

* present work.



UFP Production by Laser Pyrolysis

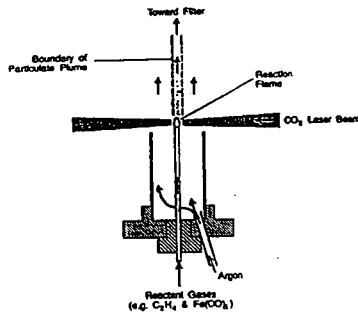


Fig. 1 Laser pyrolysis system for the synthesis of ultrafine iron carbide and sulfide particles.

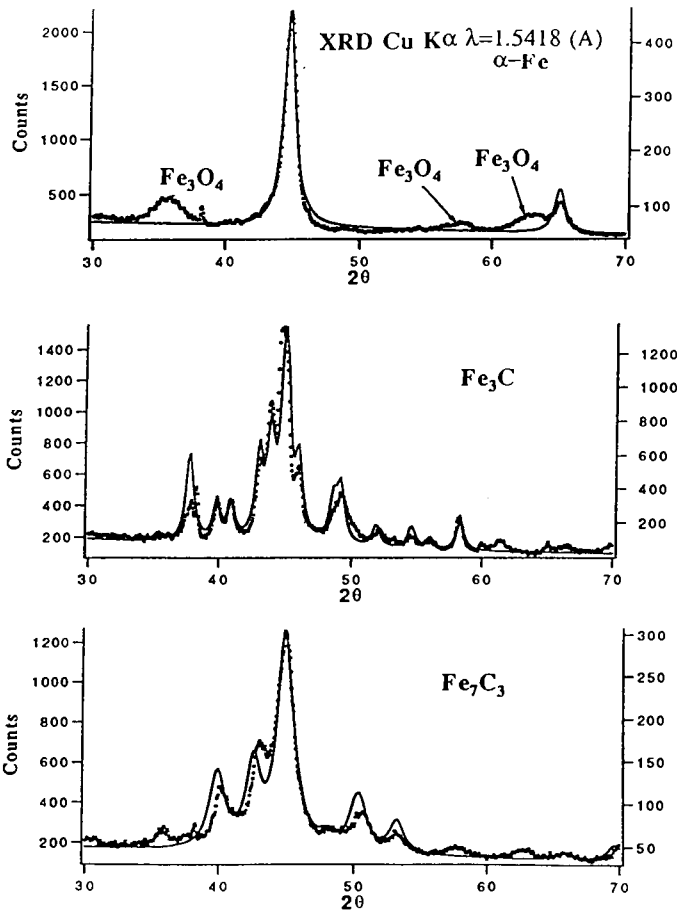


Fig. 2 XRD data(dots) for $\alpha\text{-Fe}$, Fe_3C and Fe_7C_3 UFPs and calculated results (solid curves) using standard diffraction data^[9] with an exponential background.

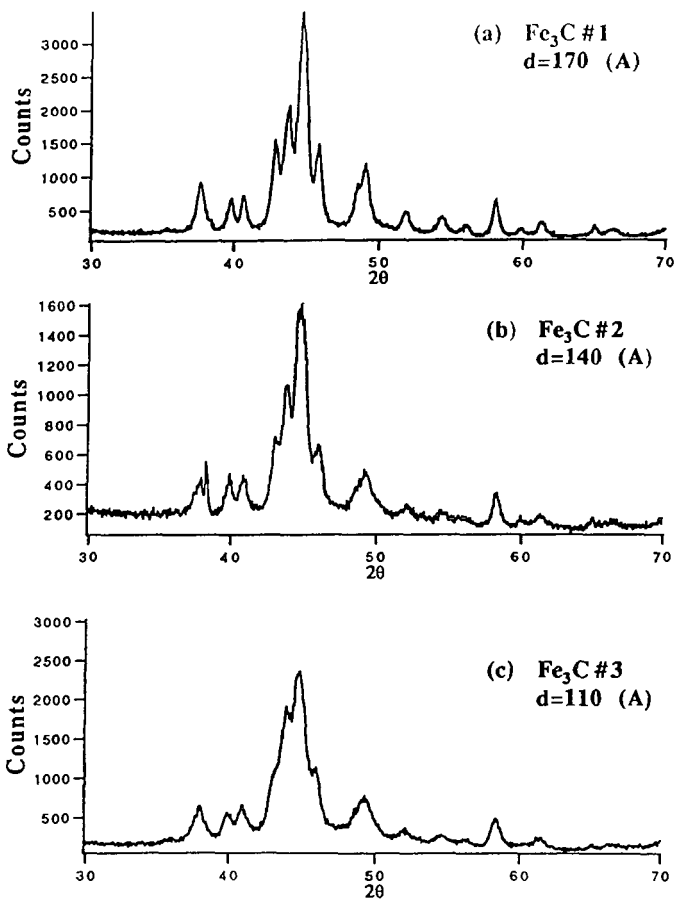


Fig. 3(a) XRD data for Fe_3C UFPs of different particle size.

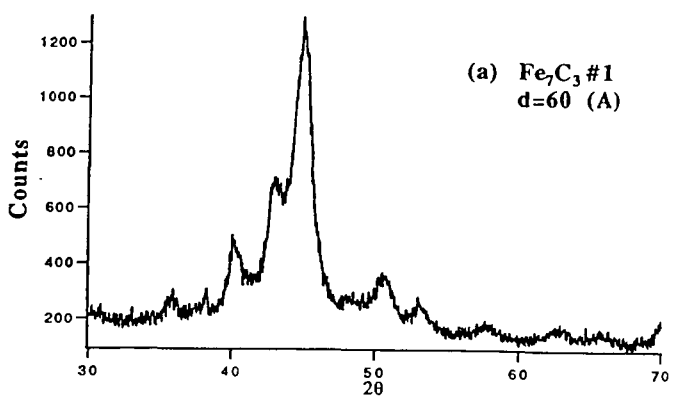
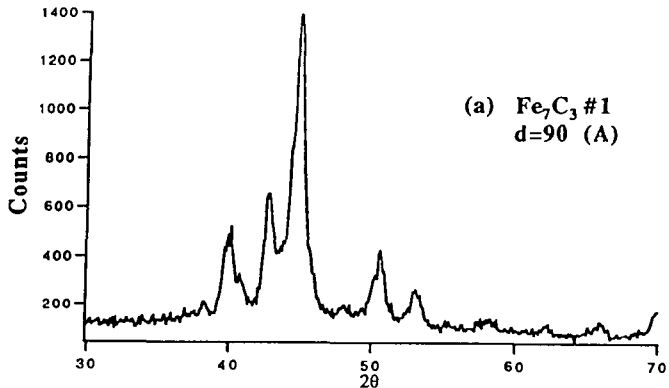


Fig. 3(b) XRD data for Fe_7C_3 UFPs of different particle size.

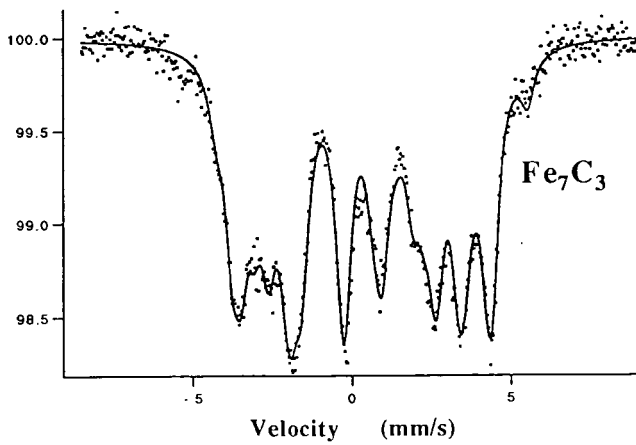
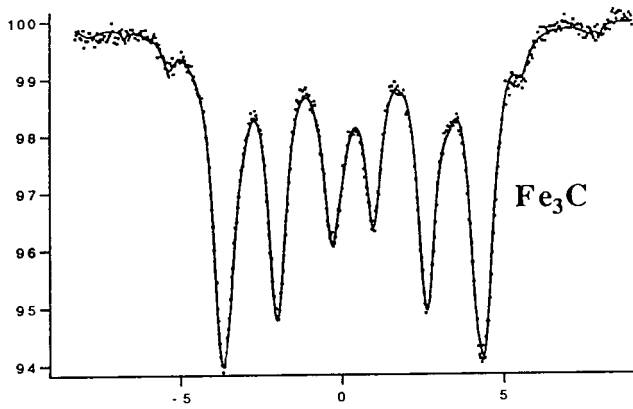


Fig. 4 ^{57}Fe Mossbauer spectra(dots) at $T=12\text{ K}$ for Fe_3C and Fe_7C_3 . Solid lines are calculated using a set of parameters that fit the data.

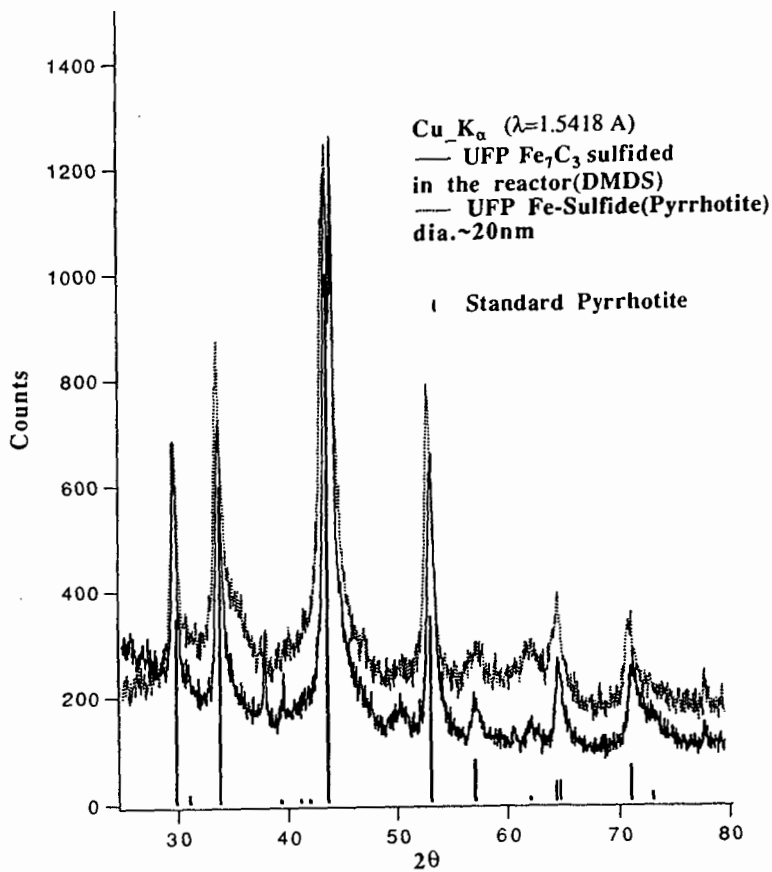


Fig. 5 Dotted lines are XRD results for the pyrrhotite Fe_{1-x}S UFPs obtained by using laser pyrolysis, and solid lines by sulfiding iron carbide Fe₇C₃ UFPs with DMDS at 375 °C(solid lines). The vertical lines represent standard powder diffraction data^[9] for Fe_{1-x}S phase.